

Disorder in DNA-Linked Gold Nanoparticle Assemblies

Nolan C. Harris and Ching-Hwa Kiang

Department of Physics and Astronomy, Rice University, Houston, TX 77005-1892

We report experimental observations on the effect of disorder on the phase behavior of DNA-linked nanoparticle assemblies. Variation in DNA linker lengths results in different melting temperatures of the DNA-linked nanoparticle assemblies. We observed an unusual trend of a non-monotonic "zigzag" pattern in the melting temperature as a function of DNA linker length. Linker DNA resulting in unequal DNA duplex lengths introduces disorder and lowers the melting temperature of the nanoparticle system. Comparison with free DNA thermodynamics shows that such an anomalous zigzag pattern does not exist for free DNA duplex melting, which suggests that the disorder introduced by unequal DNA duplex lengths results in this unusual collective behavior of DNA-linked nanoparticle assemblies.

PACS numbers: 81.07.-b, 05.70.-a, 82.70.-y, 82.70.Dd

DNA-linked nanoparticle assemblies are a novel system in which gold nanoparticles are chemically attached to known DNA sequences to create DNA "probes" with the capability to self-assemble into aggregates [1, 2, 3, 4, 5]. The interaction potential between these colloids are tunable and controllable, which makes these multicomponent complex fluids particularly suitable for studying the link between the interaction potential and phase behavior [6, 7]. Similar colloidal phase transitions have also been used to detect the protein interactions at membrane surfaces [8]. On the other hand, the dynamics of DNA melting and hybridization in DNA replication and transcription is also a subject of intense investigation [9, 10].

The change in optical property upon aggregation makes DNA-linked nanoparticle systems a potential tool in future DNA detection technology [11, 12]. DNA detection is important in medical research for applications such as detection of genetic diseases, RNA profiling, and biodefense [13, 14, 15, 16, 17]. The DNA-linked nanoparticle detection systems utilize the sequence-dependent hybridization of DNA for accuracy and the optical properties of colloidal gold for sensitivity to create a DNA detection method that changes color upon the introduction of a specific DNA sequence. Study of these DNA-gold nanoparticle assemblies is warranted to gain a fundamental understanding of DNA hybridization in confined geometries, as well as to probe the potential of this and similar systems for practical applications in biotechnology [18, 19].

Much like other colloidal suspensions [20, 21, 22], the DNA-gold nanoparticle system has been shown to exhibit interesting phase behavior. The assembly melting temperature is dependent upon parameters such as particle size, DNA composition, and electrolyte concentrations [1, 2]. Recent theory has sought to explain these observations [6, 23, 24]. More study is necessary to fully understand the underlying mechanism affecting the phase behavior of this system.

Here we report experimental observations of the effects of disorder on the melting temperature of the DNA-

linked nanoparticle assemblies [2, 3]. The basic building block is illustrated in Fig. 1. Disorder in the DNA duplex length was introduced by choosing linker DNA with an odd number of bases. We studied the melting temperature as a function of DNA linker length. The melting temperature accesses the stability of systems. DNA-gold nanoparticle probes were synthesized using previously described methods [2]. DNA-gold aggregates were formed by mixing probe DNA particles with linker DNA [2, 3, 4]. Upon the addition of linker DNA, the solutions were allowed to stand at 4 °C for several days in order to achieve maximum network aggregation.

Simple DNA sequences with uniform base composition were chosen in order to remove complications resulting from sequence-dependent effects. The probe sequences used in these experiments consisted of 11 identical bases

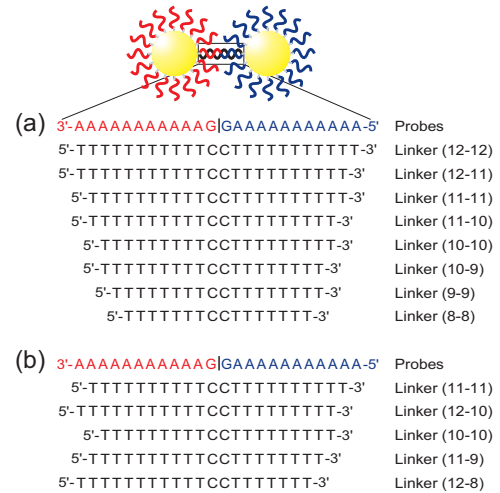


FIG. 1: (color online) Basic building block of DNA-linked gold nanoparticle aggregates. There are no bonds between the 2 G bases in the probe DNA. Linker DNA sequences used are the following: (a) sequences of varying length and (b) sequences with the same length, but different base distribution. All linkers are named such that the number of bases from the 5' end to the middle of the sequence are listed first, followed by the number of bases from the 3' end to the middle.

in a row and one "discriminator" base at the terminus that is not thiol modified (see Fig. 1). In this system, when gold-attached DNA probes aligned to bind with a specific linker sequence, the two "G" bases at the end of each probe met in the middle. These bases served to ensure that every linker sequence hybridized by aligning with the two G bases in the center. Hybridizing any other way will result in at least two base pair mismatches, which is much less stable than a fully complementary bond and, therefore, will not be present in any significant amount in our aggregates.

We chose linker DNA sequences to observe the effect of linker length on the DNA-gold nanoparticle system. Gold-attached DNA clusters were prepared using linkers that ranged from 24 to 16 bases in length. The linker concentration was adjusted to be oversaturated so the melting temperature does not depend on linker concentration [6, 25]. Typical 10 nm gold and DNA linker concentrations were 4×10^{17} particles/l and 7×10^{-6} M, respectively. Melting curves of corresponding DNA free of gold nanoparticles were measured for comparison [2, 3]. Melting of the system is observed at 260 nm, heating the solution at a rate of $1^\circ\text{C}/\text{min}$.

Experimental melting curves detailing the typical melting behavior of DNA-linked nanoparticle networks, in which linkers of varying length were used, are given in Fig. 2. From the data it is evident that the melting of these aggregates produce a sharp melting transition. More interestingly, we noticed that linker sequences with 21 and 23 bases melted at lower temperatures than linkers with 20 and 22 bases, respectively, as shown in Fig. 3(a).

To identify the cause of this anomaly in T_m , we compared the thermodynamic parameters of corresponding DNA that are not attached to gold nanoparticles. The experimental results of using free DNA counterparts in similar experimental conditions are shown in Fig. 3(a). The melting temperature of a free DNA duplex increases as the number of base pairs increases and does not display this anomaly. In contrast, the melting temperature

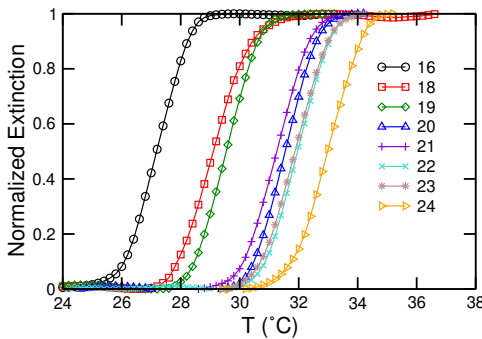


FIG. 2: (color online) Melting curves at 260nm for gold-attached DNA assemblies formed using linkers with between 16 and 24 bases.

of gold-attached DNA duplexes oscillates. T_m increases with linker length when a linker has an even number of bases and decreases when it has an odd number. This behavior is also observed on a system with a different particle size, as demonstrated in Fig. 2, where the T_m data for aggregates formed using 20 nm gold particles have a similar trend.

The melting temperatures of free DNA duplexes were predicted using experimental thermodynamic parameters. The thermodynamic relationship describing the free energy of a system is given by

$$G^0 = H^0 - TS^0 \quad (1)$$

The melting temperature of a DNA duplex is defined as the midpoint between aggregated and dispersed phases in the absorption curves [26]. At that temperature the concentration of single-stranded DNA is equal to that of double-stranded DNA. A widely used equation to calculate T_m , taking into account influence from nearest neighbor interactions and salt concentration, gives the melting temperature of a duplex as [27, 28]

$$T_m = \frac{B}{C} \frac{H^0 + 3.4 \frac{\text{kcal}}{\text{mol}}}{S^0 - R \ln \left[\frac{1}{[\text{DNA}]} \right]} + 16.6 \log_{10} ([\text{Na}^+]) \quad (2)$$

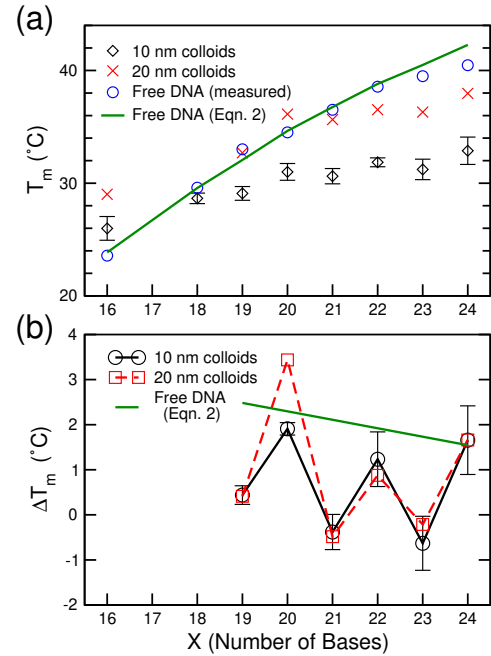
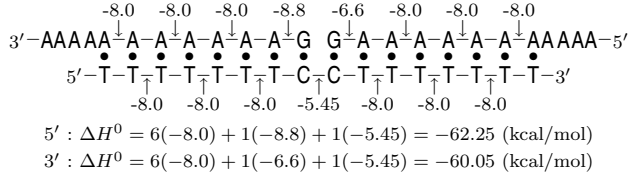


FIG. 3: (color online) (a) Melting temperature as a function of linker sequence length for free, unattached DNA, and 10 and 20 nm gold-attached DNA. Solid line represents predicted values using empirically determined thermodynamic parameters. (b) Change in melting temperature as linker sequence length increases. Values and error bars (one standard error) for 10 nm gold-attached DNA data are taken from four separate experiments.

The change in enthalpy, H^0 , and the change in entropy, S^0 , for a given DNA duplex were calculated by using nearest neighbor parameters [27, 28]. The free energy change, G^0 , was estimated using Eq. (1). A sample calculation for a DNA duplex formed using two 12 base probes and 16 base linker DNA is illustrated below.



Since the sugar-phosphate backbone of the two probe DNAs are not connected [see Fig. 1 (a)], the DNA double helix melts more like two duplexes. Therefore, a duplex formed using two 12 base probes and a 16 base linker melts at a temperature similar to that of a DNA double helix with eight base pairs. The calculated thermodynamic values are given in Table I. Figure 3(a) shows that the experimentally observed free DNA melting temperatures are described well by Eq. (2), with a deviation apparent as the DNA duplex length approaches 12 bases; it is known that Eq. (2) is accurate up to 12 bases and becomes less accurate for longer sequences [27]. In the DNA-linked nanoparticles, however, T_m does not increase monotonically with linker DNA length. Specifically, the T_m of 21 and 23 base linkers were found to be lower than that of 20 and 22 base linkers, respectively.

The T_m and associated error bars for DNA linked to 10 nm nanoparticles were determined from the averages and standard deviations from four separate data sets. The error bars are likely an overestimate of error in T_m trend because systematic error leads to a constant shift of T_m with each data set. Parameters such as salt concentration, grafting density, and linker concentration that will affect the T_m are kept constant within each data set by using the probe sample from the same batch of solution and keeping the linker concentration constant. To compare data within a given set, where systematic errors are minimized, we plot the change in melting temperature, $T_m = T_m(x) - T_m(x-1)$, versus number of bases in the linker sequence, x . Figure 3(b) demonstrates that linker lengths of 19, 21, and 23 are lower than expected, and this is true for both 10 and 20 nm nanoparticle systems. We found that the T_m decreased when increasing linker length from 20 to 21 and from 22 to 23 bases. While an increase from 18 to 19 bases does not result in a negative T_m , the T_m is near zero and significantly smaller than the predictions for free DNA.

This anomaly in T_m is unique in the DNA-linked nanoparticle system, and it does not result from the DNA duplex formation free energy, as illustrated in Fig. 2. Careful examination of the linker compositions reveals that, for linkers with an even number of bases, the DNA

duplexes formed are composed of a uniform DNA length while those with an odd number of bases form duplexes composed of two different DNA lengths. For example, a 21 base linker results in a connection composed of one 11 base and one 10 base duplex (11-10), whereas a 20 base linker results in a (10-10). While an 11 base duplex is more stable than a 10 base duplex, an assembly with the disorder introduced by the 11-10 duplex results in a lowering of the overall stability, hence the melting temperature, of the system.

To verify that introducing a different DNA duplex length, which introduces binding energy disorder, is responsible for lowering the melting temperature, we tested linkers of the same length with different sequences, as shown in Fig. 1(b). We compared three 20 base linkers, (10-10), (11-9), and (12-8). We found that T_m (10-10) > T_m (11-9) > T_m (12-8). Typical melting curves for these experiments are given in Fig. 4(a). Similar results are demonstrated for 22 base linkers, T_m (11-11) > T_m (12-10). This leads to a conclusion that, in DNA-linked nanoparticle assemblies, duplexes with different lengths introduces binding energy disorder and, therefore, lower the stability of the system. Since the energetics of corresponding free DNA duplexes do not result in such an unusual T_m trend, we believe such an effect is largely a result of entropic cooperativity [6, 25].

TABLE I: Predicted thermodynamic parameters for unattached DNA duplexes

Linker ^a	Duplex ^b	H ⁰ ($\frac{\text{kcal}}{\text{mol}}$) ^c	S ⁰ ($\frac{\text{cal}}{\text{mol}\cdot\text{K}}$) ^c	G ⁰ ($\frac{\text{kcal}}{\text{mol}}$) ^d	[DNA] (10 ⁻⁶ M) ^e	T _m ^f
16	8	60.05	162.0	11.75	7.83	23.9
	8	62.25	169.1	11.83		
18	9	68.05	183.9	13.22	6.64	29.6
	9	70.25	191.0	13.30		
19	9	68.05	183.9	13.22	6.61	32.1
	10	78.25	212.9	14.77		
20	10	76.05	205.8	14.69	6.65	34.6
	10	78.25	212.9	14.77		
21	10	76.05	205.8	14.69	6.73	36.8
	11	86.25	234.8	16.24		
22	11	84.05	227.7	16.16	6.57	38.8
	11	86.25	234.8	16.24		
23	11	84.05	227.7	16.16	6.40	40.5
	12	94.25	256.7	17.71		
24	12	92.05	249.6	17.63	6.37	42.3
	12	94.25	256.7	17.71		

^aEach linker forms two duplexes. Linkers with an even number of bases form equal length duplexes; odd numbered linkers form duplexes differing in length by one base pair.

^bThe upper row of each linker indicates length of duplex formed by starting at the 3⁰ terminus and ending in the middle; the lower row represents duplex starting from the middle to the 5⁰ terminus.

^c Calculated using experimentally determined parameters from [27].

^dC calculated using Eq. (1).

^eDetermined using optical density of duplex DNA.

\overline{T}_m is the average of the two temperatures (from the upper and lower rows) calculated using Eq. (2) with 0.3 M NaCl.

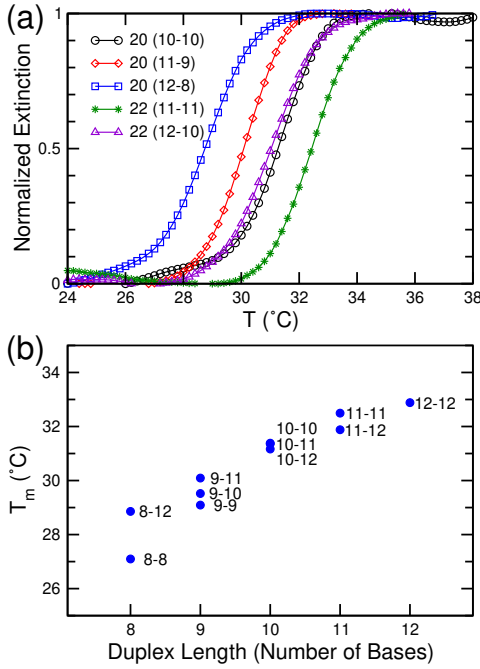


FIG. 4: (color online) (a) Melting curves at 260 nm for aggregates formed using linkers with an equal number of bases, but a different distribution of bases among the probe duplexes. (b) Melting temperature as a function of the shortest DNA duplex created using linkers of specific length and base distribution.

The effect of having two DNA duplexes of different length on the stability of DNA-linked nanoparticle assemblies is illustrated in Fig. 4(b). The stability is not simply dominated by the shorter duplex, as demonstrated in Fig. 4(b), where T_m is plotted as a function of the shorter duplex length. In the case of a DNA linker composed of one 10 base duplex, $T_m(12-10) < T_m(11-10) < T_m(10-10)$. This suggests that the larger the length difference is between the two duplexes, the less stable the aggregate will become. However, a decrease in binding energy per base has a larger percentage effect on shorter DNAs, so the unusual trend in T_m for nine base and shorter duplexes can be seen only quantitatively.

In summary, we found that disorder has a strong effect on the stability in the DNA-linked nanoparticle assemblies. We have demonstrated that using linker DNA that results in the presence of two duplexes of different length and energy in such a system lowers the overall stability of network formed. The interaction energy is easily tunable by changing the DNA composition, which makes this system particularly suitable for studying various aspects of colloidal phase transitions.

We are grateful to Royce K. P. Zia for helpful discussions. N. C. H. acknowledges the support from the Keck Center for Computational and Structural Biology of the Gulf Coast Consortia.

To whom correspondence should be addressed.

Electronic address: chkiang@rice.edu

- [1] R. Jin, G. Wu, Z. Li, C. A. Mirkin, and G. C. Schatz, *J. Am. Chem. Soc.* **125**, 1643 (2003).
- [2] C.-H. Kiang, *Physica A* **321**, 164 (2003).
- [3] Y. Sun, N. C. Harris, and C.-H. Kiang, *Physica A* **350**, 89 (2005).
- [4] Y. Sun, N. C. Harris, and C.-H. Kiang, *Physica A* **354**, 1 (2005).
- [5] Y. Sun and C.-H. Kiang, *Handbook of Nanostructured Biomaterials and Their Applications in Nanobiotechnology* (American Scientific Publishers, Stevenson Ranch, CA, USA, 2005), vol. 2, chap. VII.
- [6] D. B. Lukatsky and D. Frenkel, *Phys. Rev. Lett.* **92**, 068302 (2004).
- [7] W. B. Russel, *Nature* **421**, 490 (2003).
- [8] M. M. Baksh, M. Jaros, and J. Groves, *Nature* **427**, 139 (2004).
- [9] G. Altan-Bonnet, A. Libchaber, and O. Krichinsky, *Phys. Rev. Lett.* **90**, 138101 (2003).
- [10] Y. Zeng, A. M. Ontchikhov, and G. Zocchi, *Phys. Rev. Lett.* **91**, 148101 (2003).
- [11] J. J. Storho, R. Elghanian, R. C. Mucic, and C. A. Mirkin, *J. Am. Chem. Soc.* **120**, 1959 (1998).
- [12] C. A. Mirkin, *Inorg. Chem.* **39**, 2258 (2000).
- [13] S. A. Kushon, K. Bradford, V. Marin, C. Suhrada, B. A. Ammitage, D. McBranch, and D. Whitten, *Langmuir* **19**, 6456 (2003).
- [14] D. J. Lockhart and E. A. Winzler, *Nature* **405**, 827 (2000).
- [15] A. A. Hill, C. P. Hunter, B. T. Tsung, G. Tucker-Kellogg, and E. L. Brown, *Science* **290**, 809 (2000).
- [16] B. Zhou, P. Wirsching, and K. D. Janda, *Proc. Natl. Acad. Sci. USA* **99**, 5241 (2002).
- [17] J. Liu and Y. Lu, *Anal. Chem.* **76**, 1627 (2004).
- [18] A. K. Boal, F. Ilhan, J. E. DeRouchey, T. T. Albrecht, T. P. Russell, and V. M. Rotello, *Nature* **404**, 746 (2000).
- [19] R. Mezzenga, J. Ruokolainen, G. H. Fredrickson, E. J. Kramer, D. Moses, A. J. Heeger, and O. Ikkala, *Science* **299**, 1872 (2003).
- [20] I. Cohen, T. G. Mason, and D. A. Weitz, *Phys. Rev. Lett.* **93**, 046001 (2004).
- [21] P. Schall, I. Cohen, D. A. Weitz, and F. Spaepen, *Science* **305**, 1944 (2004).
- [22] S. Manley, L. Cipelletti, V. Trappe, A. E. Bailey, R. J. Christianson, U. Gasser, V. Prasad, P. N. Segre, M. P. Doherty, S. Sankaran, et al., *Phys. Rev. Lett.* **93**, 108302 (2004).
- [23] S. Y. Park and D. Stroud, *Phys. Rev. B* **67**, 212202 (2003).
- [24] A. V. Tkachenko, *Phys. Rev. Lett.* **89**, 148303 (2002).
- [25] A. Zilman, J. Kieffer, F. Molino, G. Porte, and S. A. Safian, *Phys. Rev. Lett.* **91**, 015901 (2003).
- [26] C. R. Cantor and P. R. Schimmel, eds., *Biophysical Chemistry, Part II: Techniques for the Study of Biological Structure and Function* (W. H. Freeman and Company, New York, 1980).
- [27] N. Sugimoto, S. Nakano, M. Yoneyama, and K. Honda, *Nucleic Acids Res.* **24**, 4501 (1996).
- [28] K. Breslauer, R. Frank, H. Blocker, and L. Marky, *Proc. Natl. Acad. Sci. USA* **83**, 3746 (1986).